Rev. Adv. Mater. Sci. 45 (2016) 76-83

TRANSMISSION OF DEFORMATION TWINS ACROSS GRAIN BOUNDARIES IN NANOCRYSTALLINE AND ULTRAFINE-GRAINED METALS

I.A. Ovid'ko[1,2,3] and A.G. Sheinerman[1,2,3]

[1]Research Laboratory for Mechanics of New Nanomaterials, Peter the Great St. Petersburg Polytechnic University, St. Petersburg 195251, Russia
[2]Saint Petersburg State University, 7/9 Universitetskaya nab., St. Petersburg, 199034, Russia
[3]Institute of Problems of Mechanical Engineering, Russian Academy of Sciences,Bolshoj 61, Vasilievskii Ostrov, St. Petersburg 199178, Russia

Received: March 12, 2016

Abstract. Transmission of nanoscale deformation twins across grain boundaries in nanocrystalline and ultrafine-grained metallic materials is theoretically described. The energy and stress characteristics of twin transmission across grain boundaries in nanocrystalline and ultrafine-grained metals are revealed. It is found that for small twin thicknesses, the critical stress for twin transmission in Cu is close to the typical values of the yield stress, and so twin transmission can actually occur in the course of deformation of nanocrystalline and ultrafine-grained Cu.

1. INTRODUCTION

Nanocrystalline and ultrafine-grained metallic materials (hereinafter called metallic nanomaterials) exhibit outstanding mechanical properties that are of utmost interest for structural and functional applications; see, e.g., [1–13]. These properties are inherent to nanomaterials due to their specific structural features – ultrasmall grains and extremely large amounts of grain boundaries (GBs) – dramatically affecting plastic deformation mechanisms in these materials. So, conventional lattice slip is limited or even completely suppressed, and deformation mechanisms assisted and/or mediated by grain boundaries (GBs) effectively operate in nanomaterials due to their specific structural features [1–13]. In particular, following numerous experimental data, computer simulations and theoretical models, nanoscale twins generated at GBs effectively contribute to plastic flow in metallic nanomaterials with various chemical compositions and structures; see, e.g., original research papers [14–23] and review [6]. In examinations of deformation twinning in nanomaterials, the main focuses were placed on generation of nanoscale twins at GBs and their growth in individual grains (e.g., [14–31]). At the same time, of utmost interest is also the transmission of nanoscale deformation twins across GBs, because this process crucially influences operation of deformation twinning in nanomaterials where amounts of GBs are very large, and it is the cooperative deformation behavior of nanoscale/ultrafine grains that is responsible for the macroscopic mechanical characteristics.

Deformation twinning often occurs in coarse-grained metals with the hexagonal close-packed (hcp) crystal structure owing to the restricted number of slip planes. In doing so, twin transmission across GBs has been experimentally observed in such hcp metals and alloys as titanium [32], mag-

Corresponding author: I.A. Ovid'ko, e-mail: ovidko@nano.ipme.ru

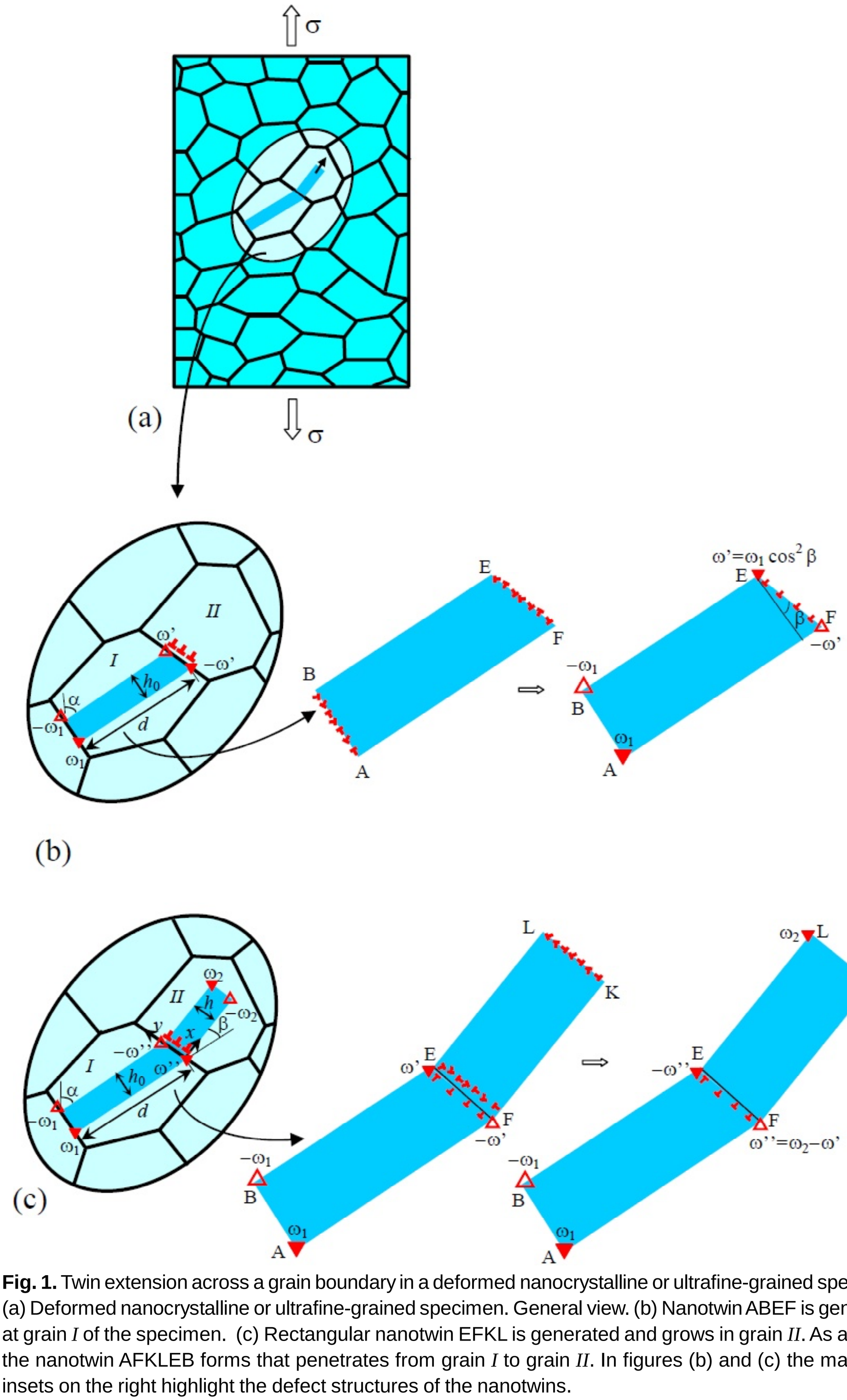

Fig. 1. Twin extension across a grain boundary in a deformed nanocrystalline or ultrafine-grained specimen. (a) Deformed nanocrystalline or ultrafine-grained specimen. General view. (b) Nanotwin ABEF is generated at grain *I* of the specimen. (c) Rectangular nanotwin EFKL is generated and grows in grain *II*. As a result, the nanotwin AFKLEB forms that penetrates from grain *I* to grain *II*. In figures (b) and (c) the magnified insets on the right highlight the defect structures of the nanotwins.

nesium alloy [33], rhenium [34], and its mechanisms have been examined in computer simulations [33]. However, deformation twinning is rarely observed in metallic nanomaterials with the hcp crystal structure, except for nanocrystalline Zr processed by surface mechanical attrition [35]. In coarse-grained metals having the face centered cubic (fcc) crystal structure, with decreasing grain size it becomes more difficult to deform by twinning [36], but twinning becomes easier once the grain size is smaller than 100 nm [37]. At the same time, deformation twinning may become difficult again when the nanograin size is too small [38]; see also a discussion of grain size effects on deformation twinning in fcc metals in review [6].

For both fcc and hcp metals, transmission of deformation twins across GBs has not been theoretically examined. Up to now, the research efforts in this area have been limited to experiments [32–34] and computer simulations [33]. At the same time, in general, theoretical analysis serves as a powerful research method capable of revealing both the general trends in the deformation processes and their specific features sensitive to the nanoscale and interface effects in nanomaterials. The main aim of this paper is to theoretically describe the conditions for transmission of deformation twins across GBs in metallic nanomaterials having the fcc crystal structure.

2. MODEL

We now consider a nanocrystalline or ultrafine-grained metallic specimen under a uniform tensile load σ (Fig. 1a). Let a deformation twin ABEF be formed in the specimen under the action of the resolved shear stress (Fig. 1b). For definiteness, we focus our examination on the typical case where the specimen has a face centered cubic (fcc) crystal lattice, and the twin lamella is bounded by two parallel coherent twin boundaries (CTBs), BE and AF, and two GB fragments, AB and EF. These GBs serve as obstacles for twin expansion. However, one can expect that, when a high enough tensile load is applied, the twin can continue its growth to adjacent grain *II* across GB (Fig. 1c). At certain conditions, the process of twin transmission across GBs to new grains can repeatedly occur, leading to macroscopic deformation twinning.

Let us calculate the critical parameters for transmission of deformation twins across GBs via the generation and motion of incoherent twin boundaries (ITBs). To do so, first, we consider the geometry and defect structure of the initial deformation twin

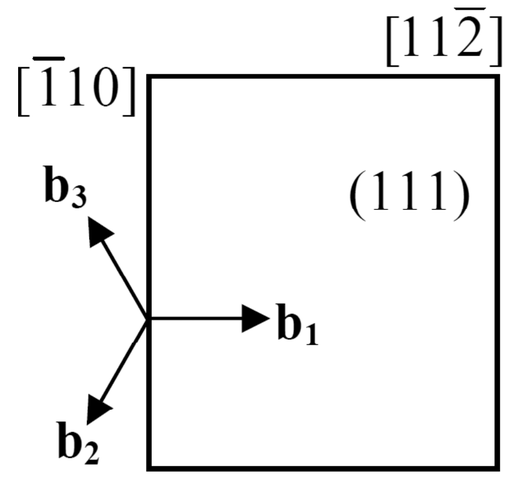

Fig. 2. Geometry of dislocations composing the incoherent twin boundary.

ABEF in the grain I (Fig. 1b). The thickness of this twin is designated by h_0, and α denotes the angle made by its CTBs BE and AF with the direction of the applied load. Also, for simplicity, we suppose that the GB fragment AB is perpendicular to the CTBs BE and AF, while the GB fragment EF makes an angle β with the normal to these GBs (Fig. 1b). The twin ABEF is bounded by two arrays of Shockley partials located at the GB fragments AB and EF. (In nanocrystalline and ultrafine-grained fcc solids, deformation twins typically form via successive or simultaneous nucleation of Shockley partials at neighboring slip planes at a GB and then by their successive or simultaneous motion to the opposite GB see, e.g., [6].) For definiteness, we suppose that the CTBs BE and AF grow along the (111) crystal planes. In these circumstances, each Shockley partial should have the line direction [$\bar{1}$10] and the Burgers vector $\pm\boldsymbol{b}_1$, $\pm\boldsymbol{b}_2$ or $\pm\boldsymbol{b}_3$, where $\boldsymbol{b}_1 = (a/6)[11\bar{2}]$, $\boldsymbol{b}_2 = (a/6)[1\bar{2}1]$, $\boldsymbol{b}_3 = (a/6)[\bar{2}11]$ (Fig. 2), and a is the crystal lattice parameter [6]. The dislocations with the Burgers vector $\boldsymbol{b}_1$ represent edge dislocations while those with the Burgers vectors $\boldsymbol{b}_2$ and $\boldsymbol{b}_3$ are 30° mixed dislocations. The vector sum of the three Burgers vectors $\boldsymbol{b}_1$, $\boldsymbol{b}_2$, and $\boldsymbol{b}_3$ is zero, that is, $\boldsymbol{b}_1 + \boldsymbol{b}_2 + \boldsymbol{b}_3 = 0$.

Due to the conservation of the dislocation Burgers vector, when a dislocation with the Burgers vector $\boldsymbol{b}_k$ (where k = 1,2,3) is generated at the GB fragment EF and moves in the adjacent grain interior, its antipode – a dislocation having the Burgers vector $-\boldsymbol{b}_k$ – is generated at the GB fragment AB. Thus, formation of the deformation twin ABEF is accompanied by the formation of the dipoles of the dislocations having the Burgers vectors $\pm\boldsymbol{b}_k$ at the GB fragments AB and EF at each (111) plane.

In general, the dislocations with the Burgers vectors $\boldsymbol{b}_k$ can produce both tilt and twist misorientations. Let us denote the fractions of the dislocations with the Burgers vectors $\boldsymbol{b}_1$, $\boldsymbol{b}_2$, and $\boldsymbol{b}_3$ as f_1, f_2, and f_3, respectively ($f_1 + f_2 + f_3 = 1$). For

simplicity, in the following, we consider the situation where, on a large scale, the additional misorientations created by the Shockley partials are constant along the GB fragments AB and EF. Also, for definiteness, we examine the twin having the zero screw component B_S of the sum Burgers vector that characterizes all the Shockley partials at the GB EF, that is, $B_S = 0$. (The latter relation holds, if $f_2 = f_3$). In the situation under consideration, for the calculation of the elastic stresses created by the dislocation walls, the two dislocation arrays AB and CD can be effectively approximated as a continuous distribution of edge dislocations having the Burgers vectors normal to the boundaries AB and CD. Following the theory of defects in solids [39], the continuous distribution of the dislocations at the GB AB can be represented as a dipole AB of wedge disclinations with the strengths $\pm\omega_1$ [39] (Fig. 1b). In doing so, the disclination strength ω_1 is defined as $\omega_1 = 2\arctan(B_e/(2h_0))$, where B_e is the edge component of the total Burgers vector of all the Shockley partials in the GB fragment AB. In turn, the quantity B_e is given as $B_e = b(f_1\text{-}f_2)h_0/p$, where $b = a/\sqrt{6}$ is the magnitude of the dislocation Burgers vectors, and $p = a/\sqrt{3}$ is the distance between the neighboring (111) crystal planes. As a result, we find the maximum possible value ω_{max} of ω_1, that is, the value corresponding to the case where $f_2 = 0$ and $f_1 = 1$, to be as follows: $\omega_{max} = 2\arctan(1/(2\sqrt{2})) \approx 39°$. The Burgers vectors of the dislocations at the wall EF make the angle β with the normal to the GB EF (see Fig. 1b). Therefore, the Burgers vectors of these dislocations can be represented as the vector sums of the components that are normal and parallel to the GB EF. In these circumstances, the dislocation ensemble at the wall EF can be imaginarily divided into two ensembles: the wall of the dislocations with the Burgers vectors normal to the GB EF, and the group of the dislocations having the Burgers vectors parallel to the GB EF.

Following the theory of defects in solids [39], the wall of the dislocations with the Burgers vectors normal to the GB EF as a stress source is equivalent to the dipole of wedge disclinations having the strengths $\pm\omega'$, where $\omega' = \omega_1\cos^2\beta$ (Fig. 1b). The density ρ of the dislocations with the Burgers vectors parallel to the GB EF (defined here as the total Burgers vector magnitude per unit length of the GB fragment EF) is given as $\rho = \omega\sin\beta\cos\beta$.

We now consider the transmission of the twin across the GB. Within our model, such transmission occurs through both the generation of a new ITB KL at the GB fragment EF and its motion across grain *II*, resulting in the formation of a new nanotwin EFKL (Fig. 1d). As with the twin ABEF, the defect structure of the new nanotwin EFKL comprises an array of the dipoles of Shockley partials located at every slip planes at the GB fragment EF and the ITB KL. Also, as with the previously considered case of the twin ABEF, we examine the twin EFKL having zero screw components of the sum Burgers vector that specifies all the newly formed Shockley partials at the GBs EF and KL. For simplicity, we also suppose that the new nanotwin region EFKL has a rectangular shape. In this case, according to the theory of defects in solids [39], the dislocation ensemble produced due to the formation and motion of the new ITB KL can be effectively approximated as a quadrupole of wedge disclinations with the strengths $\pm\omega_2$, located at the points E, F, K and L (Fig. 1c). The disclinations with the strengths $-\omega_2$ and ω_2 formed at the points E and F, respectively, due to the formation of the twin EFKL in grain *II* merge with the disclinations that belong to the twin ABEF, are located at the points E and F and have the strengths ω' and $-\omega'$, respectively. The merging produces the wedge disclinations E and F having the strengths $-\omega''$ and ω'', respectively, where $\omega'' = \omega_2 - \omega'$ (Fig. 1c). As a result of the twin transmission across GB, the defect structure is formed that consists of the disclinations with the strengths ω_1 and $-\omega_1$ at the points A and B, the disclinations with the strengths ω'' and $-\omega''$ at the points F and E, the disclinations with the strengths ω_2 and $-\omega_2$ at the points L and K, and a continuous distribution of edge dislocations specified by the density ρ at the GB fragment EF (Fig. 1d).

(Note that the formation of the quadrupole of the disclinations having the strengths $\pm\omega_2$ leads to the rotation of the GB EF by the angle $\omega_2/2$. However, in the following, we focus on the situation where the angle $\omega_2/2$ is comparatively low (up to 5°), and the effect of the rotation of the GB EF can be neglected.)

3. CRITICAL PARAMETERS FOR TWIN TRANSMISSION ACROSS A GRAIN BOUNDARY

Let us calculate the critical parameters for twin transmission across the grain boundary EF. To do so, first, we introduce the Cartesian coordinate system (x,y) with the origin at the point F, as shown in Fig. 1c, and denote the distance AF as d. (Also, d can be treated as the characteristic grain size.) In order to find the critical parameters for twin transmission across the GB EF, we have calculated the force projection F_x exerted on the moving ITB KL. The force F_x can be presented as

$$F_x = F_x^{def} - (h/p) b\tau_p^e + \tau\omega_2 h - 2\gamma_{CTB}, \quad (1)$$

where F_x^{def} is the force (per unit length of defects) exerted on the disclination dipole KL by both the disclinations at the points A, B, E, and F and the dislocation distribution at the GB fragment EF, γ_{CTB} is the specific (per unit area) energy of CTBs, $h = h_0/\cos\beta$ is the thickness of the twin EFKL, $\tau_p^e = f_1\tau_{p1} + (1 - f_1)\tau_{p2}$ is the effective Peierls stress, τ_{p1} and τ_{p2} are the Peierls stresses for the motion of the edge and mixed 30° dislocations, respectively, and $\tau = \sigma\sin[2(\alpha - \beta)/2]$ is the resolved shear stress. The first term on the right hand side of formula (1) describes the force exerted on the moving ITB by the disclinations located at the points A, B, E, and F; the second term gives the force exerted by the applied load σ; the third term determines the force related to the extension of the CTBs EL and FK in the course of the ITB motion; and the last term specifies the force associated with the Peierls barrier to the motion of the dislocations composing the moving ITB KL.

The force F_x^{def} appearing in formula (1) has been calculated based on the expressions for the stress fields of the dislocations [40] and disclinations [39] in an infinite isotropic solid. As a result, we have obtained the following final expression for the force F_x:

$$F_x = D\omega_2\left(-\omega_1 S - \omega''\left[g(0,0) - g(0,h)\right]\right) + \frac{\sigma\omega_2 h\sin\left[2(\alpha-\beta)\right]}{2} - 2\gamma_{CTB} - h\tau_e/\sqrt{2}, \quad (2)$$

where $D = G/[2\pi(1 - \nu)]$, G is the shear modulus, ν is the Poisson's ratio, x is the length of the CTBs EK and FL, $S = g(x_1,y_1) - g(x_2,y_2)$,

$$g(x_k,y_k) = \frac{1}{2}(x - x_k)\ln\frac{(x-x_k)^2 + (y_k - h)^2}{(x-x_k)^2 + y_k^2}, \quad (3)$$

$x_1 = -d\cos\beta$, $y_1 = d\sin\beta$, $x_2 = d\cos\beta + h_0\sin\beta$, and $y_2 = d\sin\beta + h_0\cos\beta$. Formula (2) accounts for the fact that the total force exerted on the moving ITB KL by the dislocations at the GB EF (with the Burgers vectors parallel to this GB) is equal to zero.

In order to calculate the critical stress for the twin transmission across a GB, we consider the most favorable case where the resolved shear stress is maximum which acts on the disclination dipole KL. In this case, we have: $\alpha = \beta + \pi/4$. We defined the critical applied load σ' as the minimum (with respect to x) value of σ at which the force F_x acting on this ITB KL is positive at any positive value of x, that is, $\min\{F_x\}|_{\sigma=\sigma'} = 0$ at $x>0$. From the latter relation and formula (2) we find:

$$\sigma' = \frac{2}{\omega_2 h}\left\{D\omega_2\left[\omega_1 M_1 + \max\left\{\left(\omega_2 - \omega_1\cos^2\beta\right)\left(g(0,0) - g(0,h)\right)\right\}\Big|_{x>0}\right] + 2\gamma_{CTB} + \frac{h\tau_p^e}{\sqrt{2}}\right\}, \quad (4)$$

where $M_1 = \max\{S\}|_{x>0}$. By considering separately the cases $\omega_2 > \omega_1\cos^2\beta$ and $\omega_2 \le \omega_1\cos^2\beta$, formula (4) can be rewritten as

$$\sigma' = \begin{cases} \sigma_1', & \omega_2 > \omega_1\cos^2\beta, \\ \sigma_2', & 0 < \omega_2 \le \omega_1\cos^2\beta, \end{cases} \quad (5)$$

where

$$\sigma_1' = \frac{2}{\omega_2 h}\left\{D\omega_2\left[\omega_1 M_1 + \left(\omega_2 - \omega_1\cos^2\beta\right)\max\left\{g(0,0) - g(0,h)\right\}\Big|_{x>0}\right] + 2\gamma_{CTB} + \frac{h\tau_p^e}{\sqrt{2}}\right\}, \quad (6)$$

$$\sigma_2' = \frac{2}{\omega_2 h}\left\{D\omega_2\left[\omega_1 M_1 + \left(\omega_2 - \omega_1\cos^2\beta\right)\min\left\{g(0,0) - g(0,h)\right\}\Big|_{x>0}\right] + 2\gamma_{CTB} + \frac{h\tau_p^e}{\sqrt{2}}\right\}. \quad (7)$$

Analysis shows that $\min\{g(0,0) - g(0,h)\}|_{x>0} = 0$. As a result, we obtain:

$$\sigma_2' = \frac{2}{\omega_2 h}\left\{D\omega_1\omega_2 M_1 + 2\gamma_{CTB} + h\tau_p^e/\sqrt{2}\right\}. \quad (8)$$

We now define the critical applied load σ_c for twin transmission across a GB as the lowest value of the stress σ' with respect to the disclination strength ω_2. The critical stress σ_c can be written as $\sigma_c = \min\{\sigma_{c1},\sigma_{c2}\}$, where $\sigma_{c1} = \min\{\sigma_1'\}|_{\omega_2 > \omega_1\cos^2\beta}$ and $\sigma_{c2} = \min\{\sigma_2'\}|_{0<\omega_2\le\omega_1\cos^2\beta}$. Since the lowest value of σ_2' in the interval $0 < \omega_2 \le \omega_1\cos^2\beta$ is reached at $\omega_2 = \omega_1\cos^2\beta$, we have: $\sigma_{c2} = \sigma_2'(\omega_2 = \omega_1\cos^2\beta) = \sigma_1'$ $(\omega_2 = \omega_1\cos^2\beta)$. As a corollary, the final expression for the critical stress σ_c can be presented in the form: $\sigma_c = \min\{\sigma_1'\}|_{\omega_2 \ge \omega_1\cos^2\beta}$.

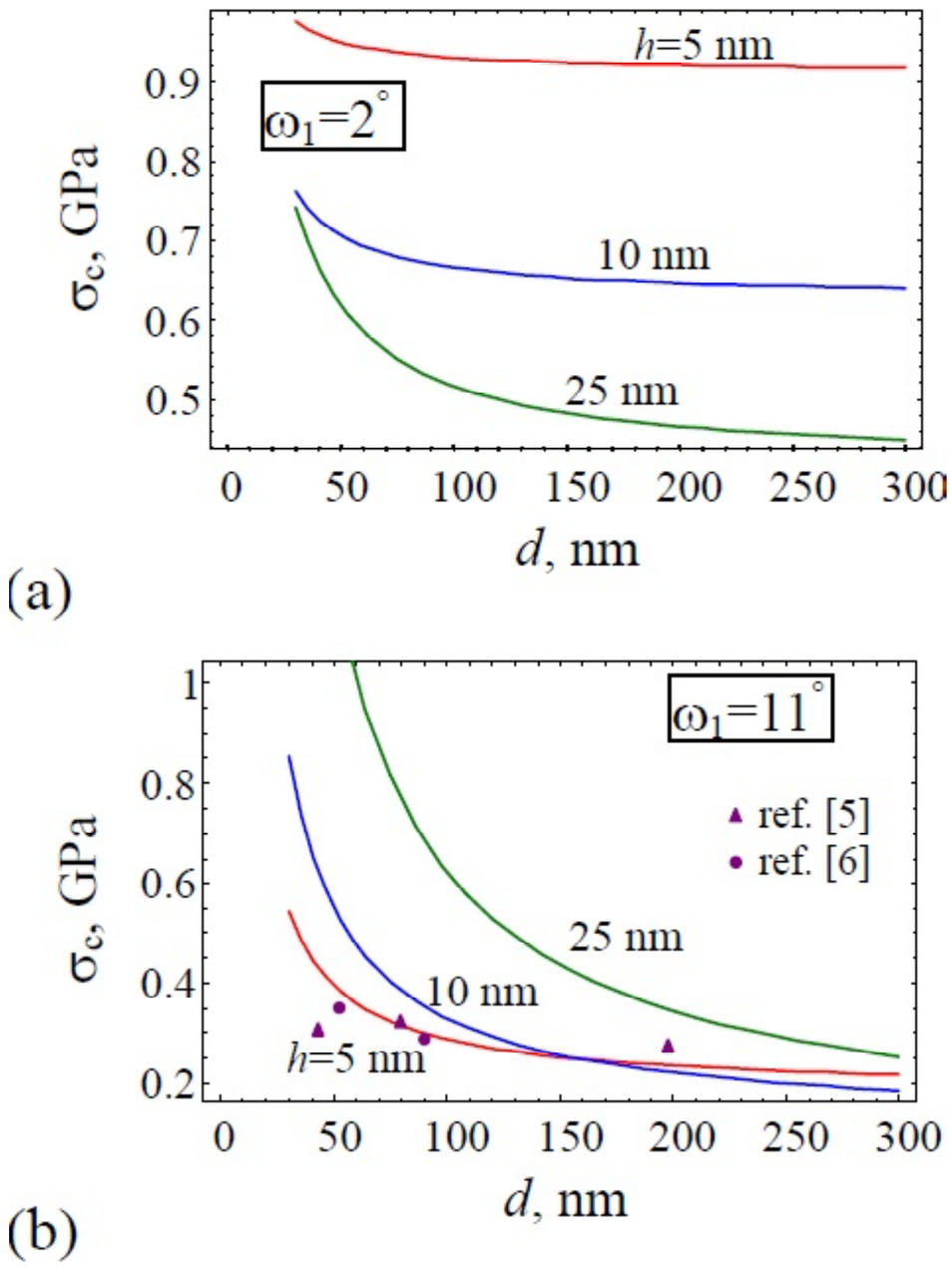

Fig. 3. Dependences of the critical applied load σ_c for twin extension across a grain boundary in nanocrystalline or ultrafine-grained Cu on grain size d, for various values of twin thickness h, $\omega_2 = 2°$ (a) and 11° (b). The circles and triangles in figure (b) show the experimental values of the yield stress for nanocrystalline and ultrafine-grained Cu.

Let us estimate the critical stress σ_c in the exemplary case of nanocrystalline and ultrafine-grained Cu characterized by the following parameter values: G = 48 GPa, ν = 0.34, and γ_{CTB} = 24 mJ/m^2 [41]. Since the exact values of the quantities τ_{p1} and τ_{p2} for Cu at room temperature are unknown, for simplicity, we put τ_p^e = 5 MPa, independent of the fraction f_1 of edge dislocations in the moving ITB.

The dependences of the critical stress σ_c on the grain size d are shown in Fig. 3, for the case $\beta = \pi/6$ and various values of the parameters h and ω_1. Fig. 3 demonstrates that σ_c decreases with increasing the grain size d. At the same time, the dependences of σ_c on twin thickness h and disclination strength ω_1 are more complicated: σ_c can either increase or decrease with rising h or ω_1. In Fig. 4, the critical stress σ_c is shown as a function of the disclination strength ω_1, for d = 100 nm and various values of twin thickness h. Fig. 4 demonstrates that the dependences $\sigma_c(\omega_1)$ have minima. With increasing h, the value of ω_1, corresponding to the point of minimum at the curve $\sigma_c(\omega_1)$, decreases, while the minimum value of σ_c increases.

The dependences of the critical stress σ_c on twin thickness h are presented in Fig. 5, for the case $\beta = \pi/6$ and various values of the parameters d and ω_1. Fig. 5 clearly shows that there always exists some equilibrium value of twin thickness h that corresponds to a minimum of σ_c. This equilibrium twin thickness increases with increase in grain size d and/or decrease in the disclination strength ω_1. Also, figures 3 to 5 show that at sufficiently small values

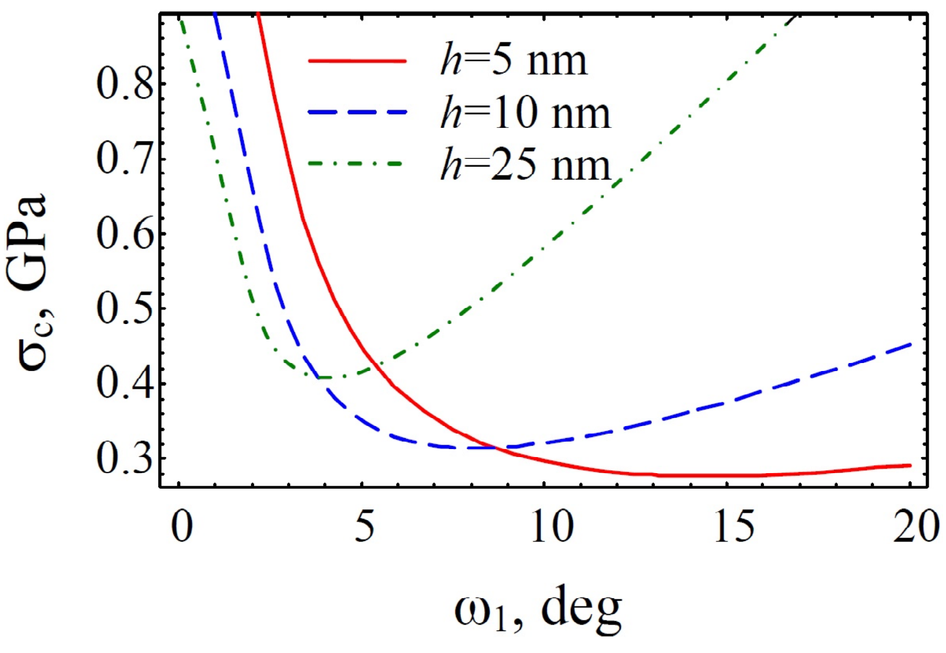

Fig. 4. Dependences of the critical applied load σ_c for twin extension across a grain boundary in ultrafine-grained Cu on disclination strength ω_1, for d = 100 nm and various values of twin thickness h.

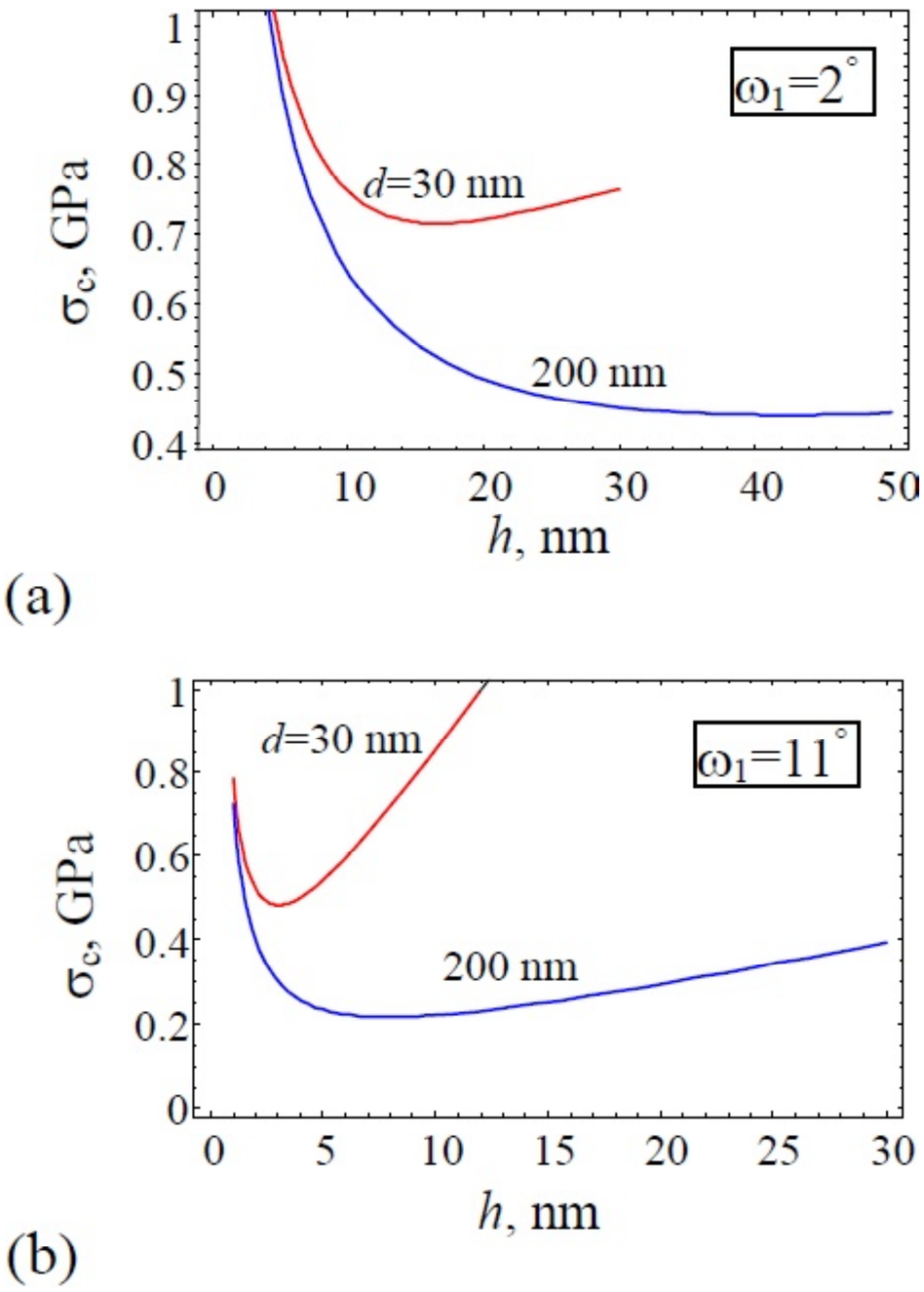

Fig. 5. The critical applied load σ_c for twin transfer across a grain boundary in nanocrystalline or ultrafine-grained Cu vs twin thickness h, for various values of grain size d, $\omega_1 = 2°$ (a) and 11° (b).

of h (around 5 to 10 nm) and ω_1, the critical stress σ_c decreases with ω_1 and, in the case $\omega_1 = 11°$ illustrated in Figs. 3b and 5b, the values of σ_c lie in the interval of 0.2–0.5 GPa for the grain size ranging from 50 to 300 nm. As it follows from Fig. 3b, these values are close to typical values [42,43] of the yield stress for nanocrystalline and ultrafine-grained Cu. As a corollary, the transmission of deformation twins across GBs can occur in nanocrystalline and ultrafine-grained Cu during plastic deformation.

4. CONCLUSIONS

Thus, in this paper, we have suggested a model for twin transmission across grain boundaries in deformed nanocrystalline and ultrafine-grained metals with the fcc lattices. The calculations demonstrated that the transmission is favored when the value of the applied load exceeds a critical stress σ_c. The critical stress decreases with increasing the grain size d and has a minimum at a certain value of twin thickness h. This value of twin thickness h increases with grain size d. For the case of Cu, the values of the critical stress σ_c are close to the typical values of the yield stress for nanocrystalline and ultrafine-grained Cu, provided that the twin is sufficiently thin and the grain size exceeds 50 nm (Fig. 3b). This means that twin transmission can indeed occur in the course of deformation of nanocrystalline and ultrafine-grained Cu. At the same time, twin transmission across GBs has been experimentally observed only in hcp metals and alloys [32–34]. Thus, further experimental observations are required to confirm the possibility for twin transmission across GBs in nanocrystalline and ultrafine-grained metals with the fcc crystal lattices.

ACKNOWLEDGEMENTS

The work was supported by the Russian Ministry of Education and Science (Zadanie 9.1964.2014K and grants 14.B25.31.0017 and MD-2893.2015.1) and the Russian Fund of Basic Research (grant 15-31-20095).

REFERENCES

[1] C.C. Koch // *J. Mater. Sci.* **42** (2007) 1403.
[2] M. Kawasaki and T.G. Langdon // *J. Mater. Sci.* **42** (2007) 1782.
[3] I.A. Ovid'ko // *J. Mater. Sci.* **42** (2007) 1694.
[4] M. Dao, L. Lu, R.J. Asaro, J.T.M. De Hosson and E. Ma // *Acta Mater.* **55** (2007) 4041.
[5] J.R. Greer and J.T.M. De Hosson // *Prog. Mater. Sci.* **56** (2011) 654.
[6] Y.T. Zhu, X.Z. Liao and X.-L. Wu // *Prog. Mater. Sci.* **57** (2012) 1.
[7] R.Z. Valiev, I. Sabirov, A.P. Zhilyaev and T.G. Langdon // *JOM* **64** (2012) 1134.
[8] M.S. Senthil Kumar, N. Mohana Sundara Raju, P.S. Sampath and L.S. Jayakumari // *Rev. Adv. Mater. Sci.* **38** (2014) 40.
[9] A.L. Stepanov, A.N. Golubev, S.I. Nikitin and Y.N. Osin // *Rev. Adv. Mater. Sci.* **38** (2014) 160.
[10] I.A. Ovid'ko // *Rev. Adv. Mater. Sci.* **38** (2014) 190.
[11] V.G. Konakov, O. Yu. Kurapova, N.N. Novik, S.N. Golubev, A.V. Osipov, A.S. Graschenko, A.P. Zhilyaev, S.N. Sergeev and I.Yu. Archakov // *Rev. Adv. Mater. Sci.* **39** (2014) 1.
[12] I.A. Ovid'ko and A.G. Sheinerman // *Rev. Adv. Mater. Sci*. **39** (2014) 99.
[13] I.A. Ovid'ko // *Phil. Trans. R. Soc.* A **373** (2015) 20140129.
[14] M. Chen, E. Ma, K.J. Hemker, H. Sheng, Y. Wang and X. Cheng // *Science* **300** (2003) 1275.
[15] X.Z. Liao, F. Zhou, E.J. Lavernia, D.W. He and Y.T. Zhu // *Appl. Phys. Lett.* **83** (2003) 5062.
[16] Y.M. Wang, A.M. Hodge, J. Biener, A.V. Hamza, D.E. Barnes, K. Liu and T.G. Nieh // *Appl. Phys. Lett.* **86** (2005) 101915.
[17] X.-L. Wu and Y.T. Zhu // *Appl. Phys. Lett.* **89** (2006) 031922.
[18] Y.T. Zhu, X.Z. Liao and X.-L. Wu // *JOM* **60** (2008) 60.
[19] Y.T. Zhu, X.-L. Wu, X.Z. Liao, J. Narayan, S.N. Mathaudhu and L.J. Kecskes // *Appl. Phys. Lett.* **95** (2009) 031909.
[20] Y.T. Zhu, J. Narayan, J.P. Hirth, S. Mahajan, X.-L.Wu and X.Z. Liao // *Acta Mater.* **57** (2009) 3763.
[21] I.A. Ovid'ko // *Appl. Phys. Lett.* **99** (2011) 061907.
[22] X.-L. Wu, K.M. Youssef, C.C. Koch, S.N. Mathaudhu, L.J. Kecskes and Y.T. Zhu // *Scr. Mater.* **64** (2011) 213.
[23] I.A. Ovid'ko and N.V. Skiba // *Scr. Mater.* **71** (2014) 33.
[24] M.Yu. Gutkin, I.A. Ovid'ko and N.V. Skiba // *Philos. Mag.* **88** (2008) 1137.
[25] N.F. Morozov, I.A. Ovid'ko, A.G. Sheinerman and N.V. Skiba // *Rev. Adv. Mater. Sci.* **32** (2012) 75.
[26] N.F. Morozov, I.A. Ovid'ko and N.V. Skiba // *Rev. Adv. Mater. Sci.* **37** (2014) 29.

[27] I.A. Ovid'ko and N.V. Skiba // *Int. J. Plasticity* **62** (2014) 50.
[28] I.A. Ovid'ko and A.G. Sheinerman // *Rev. Adv. Mater. Sci.* **39** (2014) 9.
[29] I.A. Ovid'ko, N.V. Skiba and A.G. Sheinerman // *Rev. Adv. Mater. Sci.* **43** (2015) 38.
[30] S.V. Bobylev, N.F. Morozov and I.A. Ovidko // *Rev. Adv. Mater. Sci.* **41** (2015) 1.
[31] I.A. Ovid'ko and N.V. Skiba // *Rev. Adv. Mater. Sci.* **43** (2015) 22.
[32] L. Wang, P. Eisenlohr, Y. Yang, T.R. Bieler and M.A. Crimp // *Scr. Mater.* **63** (2010) 827.
[33] A. Fernández, A. Jérusalem, I. Gutiérrez-Urrutia, M.T. Pérez-Prado // *Acta Mater.* **61** (2013) 7679.
[34] J. Kacher and A.M. Minor // *Acta Mater.* **81** (2014) 1.
[35] L. Zhang and Y. Han // *Mater. Sci. Eng.* A **523** (2009) 130.
[36] M.A. Meyers. O. Vohringer and V.A. Lubarda // *Acta Mater.* **49** (2001) 4025.
[37] V. Yamakov, D. Wolf, S.R. Phillpot, A.K. Mukherjee and H. Gleiter // *Nature Mater.* **1** (2002) 45.
[38] X.L. Wu and Y.T. Zhu // *Phys. Rev. Lett.* **101** (2008) 025503.
[39] A.E. Romanov and V.I. Vladimirov, In: *Dislocations in Solids*, vol. 9, ed. by F.R.N. Nabarro (North Holland, Amsterdam, 1992), p. 191.
[40] J.P. Hirth and J. Lothe, *Theory of Dislocations* (Wiley, New York, 1982).
[41] R. Niu and K. Han // *Scr. Mater.* **68** (2013) 960.
[42] P.G. Sanders, J.A. Eastman and J.A. Weertman, In: Processing and Properties of Nanocrystalline Materials, ed. by C. Suryanarayana, J. Singh and F.H. Froes (Warrendale, PA, TMS, 1996), p. 379.
[43] R. Suryanarayama, C.A. Frey, S.M.L. Sastry, B.E. Waller, S.E. Bates and W.E. Buhro // *J. Mater. Res.* **11** (1996) 439.